CrossMark

ORIGINAL ARTICLE

A short-term test method to determine the chloride threshold of steel–cementitious systems with corrosion inhibiting admixtures

Jayachandran Karuppanasamy · Radhakrishna G. Pillai

Abstract Now-a-days, multiple types of corrosion inhibiting admixtures (CIAs) are being used to enhance the chloride threshold (Cl_{th}) of steel–cementitious systems. However, due to the application of external potential to drive chlorides, some existing short-term test methods are not suitable to assess the Cl_{th} of S–C systems with CIAs containing anions. This paper presents the development of a Modified Accelerated Chloride Threshold (mACT) test to determine the Cl_{th} for S–C systems with CIAs. The test specimens consisted of a mortar cylinder with an embedded steel piece and electrodes forming a 3-electrode corrosion cell. The specimens were exposed to chloride solution and the linear polarization resistance tests were conducted every 3.5 days. The corrosion initiation was detected using statistical analysis of the repeated R_p measurements. After corrosion initiation, the chloride content in mortar adjacent to the embedded steel piece was determined and defined as Cl_{th}. The time required to complete mACT test for an S–C system with CIAs is about 120 days. The Cl_{th} of eight specimens each with S–C system containing (i) without inhibitor, (ii) anodic inhibitor [calcium nitrite] and (iii) bipolar inhibitor [both calcium nitrite and amino alcohol] were determined. Both anodic and bipolar CIAs showed enhanced corrosion resistance. Also, the bipolar inhibitor performed better than anodic inhibitor. It was concluded that the use of CIAs could significantly delay the initiation of chloride-induced corrosion. The mACT test can be used to determine the Cl_{th} and estimate the service life during the planning and design stages of a project and help select durable materials.

Keywords Chloride threshold · QST steel · Corrosion inhibitor · Calcium nitrite · Bipolar inhibitor

List of abbreviations

%bwoc	% by weight of cement
σ_5	Standard deviation of R_p data set considered for analysis
σ_{st}	Standard deviation of stable R_p data set
ACT	Accelerated threshold test
AN	Anodic inhibitor
BP	Bipolar inhibitor
CIA	Corrosion inhibiting admixtures
Cl_{th}	Chloride threshold value (%bwoc)
C_s	Surface chloride concentration
D_{cl}	Chloride diffusion coefficient of concrete (m^2/s)
E	Applied potential (Volt)
E_{corr}	Corrosion potential (millivolt)
EIS	Electrical Impedance Spectroscopy
I	Corrosion current (milliampere)
ISE	Ion specific electrode

J. Karuppanasamy · R. G. Pillai (✉)
Department of Civil Engineering, Indian Institute of
Technology Madras, Chennai, India
e-mail: pillai@iitm.ac.in

rilem

k	Multiplication coefficient to define stable data
LPR	Linear polarization resistance
mACT	Modified accelerated chloride threshold
$M(t_i)$	Median of time required for t_i (year)
OCP	Open circuit potential
OPC	Ordinary portland cement
PDF	Probability density function
QST	Quenched and self-tempered
R_{cm}	Resistance of cementitious system ($\Omega\ cm^2$)
RCPT	Rapid chloride permeability test
RMT	Rapid migration test
R_p	Polarization resistance at steel–cementitious interface ($\Omega\ cm^2$)
R_{total}	Bulk resistance of steel–cementitious system ($\Omega\ cm^2$)
SCE	Saturated calomel electrode
SPS	Simulated pore solution
t	Duration of exposure (year)
t_i	Time required for corrosion initiation (year)
x	Depth considered to determine anion concentration (mm)

1 Introduction

1.1 Chloride threshold (Cl$_{th}$)

The chloride threshold (Cl$_{th}$) is one of the key input parameters for service life estimation models. A small change in the Cl$_{th}$ value may have a significant influence on the estimated service life [1–4]. When a structure is exposed to marine environment, chloride ions can diffuse through the concrete cover and reach the steel reinforcement. Once they come in contact with the steel reinforcement and build up in sufficient quantity, they damage the protective, passive film (even at high pH) and initiate active corrosion [5–7]. The Cl$_{th}$ can be defined as the minimum concentration of chlorides required at the rebar level to initiate corrosion, irrespective of the high pH level [8]. Significant research has been done to quantify the Cl$_{th}$ of various types of steel reinforcement embedded in concrete. Angst et al. [9] provided a thorough state-of-the-art review on Cl$_{th}$. Figure 1 shows the Cl$_{th}$ values (based on laboratory results) reported in the literature. These values exhibit a huge scatter and vary
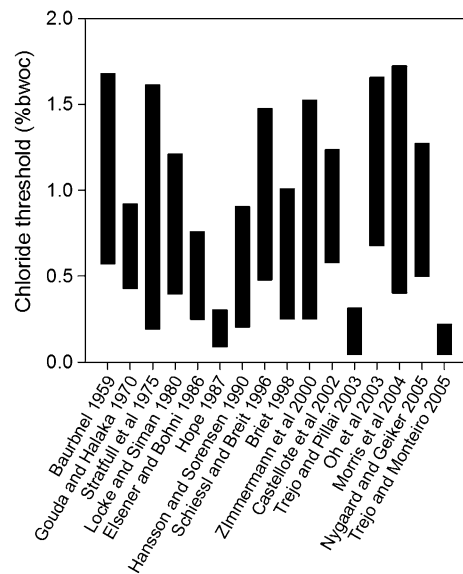

Fig. 1 Chloride threshold values reported in literature

from 0.1 to 1.8% by weight of cement (%bwoc). This scatter may be due to the variations in the influencing factors like binder type, water-binder ratio, steel type, exposure conditions, etc. Also, the differences in the test methods followed by different researchers to detect the corrosion initiation may be another cause for the scatter among the reported values of Cl$_{th}$. Hence, a reliable short-term test method that can be standardized is required to determine the Cl$_{th}$ of steel–cementitious systems (S–C), especially with corrosion inhibiting admixtures (CIAs).
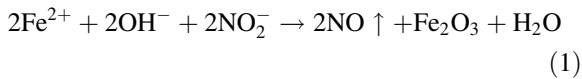
1.2 Corrosion inhibiting admixtures (CIAs)

The CIAs offer an economical and easier way to increase the Cl$_{th}$ of steel embedded in concrete [5, 10–14]. A variety of CIAs are available in the market. Calcium nitrite [Ca(NO$_2$)$_2$] is a widely used anodic CIA. Also, the bipolar CIAs are emerging in the construction industry. Following is a discussion on anodic (AN) and bipolar (BP) inhibitors.

1.2.1 Anodic inhibitor (AN)

Various authors reported that the AN inhibitor enhanced the corrosion resistance in alkaline environments compared to other CIAs [15–17]. For example, the calcium nitrite inhibitor helps in forming a better

passive film based on the reactions in Eqs. 3 and 4 [5, 17].

$$2Fe^{2+} + 2OH^- + 2NO_2^- \rightarrow 2NO \uparrow + Fe_2O_3 + H_2O \tag{1}$$

$$Fe^{2+} + OH^- + NO_2^- \rightarrow NO \uparrow + \gamma FeOOH \tag{2}$$

At the anode, ferrous ion (Fe^{2+}) ions (as soon as they form) are oxidized to ferric ions (Fe^{3+}), which are very stable in the nitrite-rich environment. Also, the nitrite ions help in producing $\gamma FeOOH$, which are more stable than naturally formed passive layer and help in increasing the Cl_{th} value. These reactions form the basis for the inhibitive action by nitrites. However, there exist mixed opinions on the effectiveness of nitrite based anodic inhibitors.

For example, it is reported that the effectiveness of the anodic inhibitor could depend on the amount of chloride ions present in the surrounding concrete [17]. It was also found that the calcium nitrite based CIAs are not effective when chloride-to-nitrite ratio (Cl^-/NO_2^-) is less than one [18]. Ann and Song found that CIAs are not suitable for concrete in immersed conditions, because the nitrite ions can leach out of the concrete and reduce the nitrite ion concentration inside the concrete [6]. The adverse effect of this leaching on corrosion depends on the quality and thickness of the cover depth—the less the quality and cover depth, the more would be the adverse effects. Supporting this, Montes et al. [19] reported that the effectiveness of calcium nitrite based CIA is seen only in concrete with low water to binder ratio (i.e., <0.5) indicating high quality cover. Note that there is a possibility for the beneficial effects of the nitrite inhibitor to decrease over the service life of the structure, due to the emission of NO, according to Eqs. (1) and (2). However, the rate of emission and its effects have to be quantified experimentally using a long-term experiment and is out of the scope of this article. Although there are ambiguities regarding the performance of calcium nitrite based CIAs, it is still one of the most widely used CIAs. Also, quantitative and probabilistic information on their effect on Cl_{th} is required for realistic estimation of service life.

1.2.2 Bipolar inhibitors (BP)

Bipolar inhibitors retard the corrosion process at both anodic and cathodic sites of a corrosion cell. The BP inhibitor acts by reducing the rate of ferrous decomposition at the anodic site and at the same time restricts the availability of oxygen at the cathodic site [20]. BP inhibitors with polar group with Nitrogen (:N), Alkyl (R), and hydroxyalkyl (R–OH) are found to be effective in inhibiting corrosion [21]. Organic polymer compounds such as amine and amino alcohol are commonly used in BP inhibitors. Rakanta et al. [22] reported that the use of organic inhibitors of 2% by weight of cement (%bwoc) could reduce the mass loss of steel by about 43%. Also, the overall performance of organic BP inhibitors in reducing the corrosion rate was better than the calcium nitrite based AN inhibitor. Nmai et al. [23] compared the performance of reinforced concrete slabs with organic and calcium nitrite inhibitors. Active corrosion was observed on control specimens (i.e., without inhibitors) after 30 days of continuous exposure to 6% chloride solution. At 50 days of exposure, the specimens containing calcium nitrite inhibitor showed active corrosion and those with organic inhibitors showed no signs of corrosion. As these types of BP inhibitors were evolved recently, very limited quantitative and the probabilistic information is available on their performance. Such information is required for the realistic estimation of service life.

1.3 Methods to detect corrosion initiation

The method of detecting the corrosion initiation can influence significantly the estimation of Cl_{th} [24]. During the 1950's, non-destructive test methods were developed to assess the electrochemical properties of steel embedded in concrete [25]. Since then, the half-cell potential and linear polarization resistance (LPR) techniques have become very popular in detecting corrosion initiation.

The ASTM C876 [26] is commonly used to find the probability of occurrence of corrosion using the corrosion potential (E_{corr}) measured. E_{corr} is a thermodynamic parameter and will not provide details about the corrosion kinetics (say, corrosion rate, i_{corr}) of the steel. Pour Ghaz et al. [24] showed that, for the same i_{corr}, the measured E_{corr} can vary with the difference in the cover concrete resistivity. In a laboratory study, Cigna et al. [27] studied the polarization resistance of the S–C interfaces (R_p) and concluded that the E_{corr} is not as good as a parameter like i_{corr} to detect the corrosion initiation.

Since the 1970s, LPR technique has been accepted as a commonly used test method to measure the instantaneous corrosion rate in the solution electrolytes with low electrical resistance. The three-electrode LPR technique given in ASTM G59 can be used to measure the polarization resistance of the S–C interface (R_p), and hence; the kinetics or rate of corrosion [28]. The LPR test setup consists of a corrosion cell with a working electrode (WE), a counter electrode (CE), and a reference electrode (RE). However, when concrete or mortar with fine pores and high bulk electrical resistance (say, ranging from 0.01 to 100 kΩ cm^2) is used as an electrolyte, it will have a major influence on the measurement of corrosion [29, 30].

Table 1 provides a list of criterion used by several researchers in detecting corrosion initiation. The data are tabulated in the form of criteria with a combination of the following:

- E_{corr} (mV; measured using half-cell potential test)
- i_{corr} (μA/cm^2; measured using LPR test)
- I_{corr} (μA; measured using galvanostatic pulse method), and
- R_p (Ω cm^2) measured using LPR test.

For example, Xu et al. [31] detected corrosion initiation using a "and/or" combination of E_{corr}, i_{corr}, and R_p and then determined the Cl$_{th}$. Bouteiller et al. [32] concluded that among E_{corr} and i_{corr} data, the i_{corr} provides more detailed and reliable information on the corrosion initiation. Also, the corrosion initiation have been defined based on (i) threshold E_{corr}, (ii) a threshold i_{corr}, (iii) a significant change in E_{corr}, (iv) a significant change in i_{corr}. However, the scatter in the corrosion data can still lead to difficulties in detecting

corrosion initiation during the experiments with repeated measurements, as is the case with the current study. As reported by Angst et al. [33], a test method that monitors the corrosion level and differentiates the stable corrosion level, significant variation in the rate during corrosion initiation of individual specimen is required. Valipour et al. [34] suggested to use the change in trend of the data obtained from real-time corrosion data using any of the above method is reliable. The current study will develop such a corrosion detection methodology using LPR technique.

1.4 Existing test methods to determine Cl$_{th}$ of steel in systems with CIAs

The Japanese Industrial Standard JIS A6205 provides a test procedure for assessing the performance of CIAs used in concrete [35]. In this method, a bare steel specimen is kept directly in contact with the simulated pore solution (SPS) or saline water (i.e., immersed in salt water) and the corrosion initiation is detected by visual observation. Poursaee reported that the corrosion performance of steel immersed in solution might be different from that embedded in concrete [36]. Therefore, the results from JIS A6205 test may not replicate the performance of steel reinforcement embedded in mortar or concrete. On the other hand, the ASTM G109 [37] test method uses measurements on steel rebars embedded in the cementitious system—mimicking the situations in real structures. This method suggests assessing the efficiency of CIAs based on the changes in the half-cell potential value [26] and macrocell corrosion current measurements during the cyclic wet-dry exposure using 3.5% sodium

Corrosion initiation criteria	References
$E_{corr} < -350$ V vs CSE and/or $i_{corr} > 0.2$ μA/cm^{-2} and/or $R_p > 10^4$ Ω cm^2	[30]
$R_p \approx 10^3$–10^4 Ω cm^2	[53]
$E_{corr} < -350$ mV vs CSE	[54]
$E_{corr} < -350$ mV vs CSE or $R_p \approx 10^3$–10^4 Ω cm^2	[31]
Two consecutive $i_{corr} > 10$ μA or $E_{corr} < -280$ mV vs SCE	[55]
Change in $E_{corr} > -200$ mV and then continue to be more negative	[33]
$E_{corr} < -350$ V vs CSE and/or $i_{corr} > 0.2$ μA/cm^{-2}	[32]
$i_{corr} > 10$ μA and $i_{corr} > 0.5$ μA/cm^2 and $E_{corr} < -233$ mV Vs (Ag/AgCl)	[34]
$i_{corr} > 15$ μA	[56]
$i_{corr} > 3\sigma$ of previous i_{corr} readings	[39]

Table 1 Corrosion initiation criteria used in literature

chloride solution. However, this test does not provide direct guidance on the determination of Cl_{th}. However, many researchers have used this method for monitoring corrosion performance and followed by further tests on the same specimens to determine Cl_{th}. It should be noted that the better the CIA, the more will be the duration of this test. Depending on the system, it may take many years to complete the ASTM G109 testing, which is not acceptable by most of the engineers, designers, and clients, who want to select the materials during the planning and design stage itself.

To overcome these issues, Trejo and Miller developed and patented an accelerated chloride threshold (ACT) test method to detect the corrosion initiation in plain cementitious systems [38]. Later, Trejo and Pillai refined the test method [39]. In this ACT test method, an external potential (20 V) is applied across the 38 mm thick mortar cover to drive the chlorides towards the embedded steel surface. This application of potential was found to be an issue in adopting this method for determining the Cl_{th} of S–C systems with CIAs.

1.5 Issues in adopting ACT test method in evaluating the performance of CIAs

The ACT test method was developed for steel embedded in plain cementitious systems and uses an external potential gradient of 20 V to accelerate the movement of chlorides towards the embedded steel in plain cementitious systems [39]. When external potential is applied, the hydroxides in the mortar can move towards the steel reinforcement and can have an effect on corrosion measurements. Also, when the mortar contains CIAs with anions (say, nitrites), the external potential can drive both the chlorides and nitrites towards the embedded steel. This can increase the nitrite concentration at the S–C interface during the testing. In other words, the nitrite concentration at the S–C interface at the beginning and after some time of testing would be different. Such increase in nitrite concentration, in turn, reduces the Cl^-/NO_2^- ratio at the S–C interface. However, such increase in the nitrite concentration at the S–C interface does not occur in real structures. Therefore, a test method that does not induce changes in nitrite concentration at the S–C interface during the course of chloride exposure and testing is required. One option would be to develop a method that does not use an external potential to drive the chlorides towards the embedded steel.

2 Research significance

Now-a-days, Corrosion Inhibiting Admixtures (CIAs) based on various chemical families are being used in concrete structures. Engineers want to quantify (during the planning and design stage itself) the effect of such CIAs on the service life of concrete structures. For this, the Cl_{th} of S–C systems with CIAs needs to be determined. However, no suitable, short-term test methods are available to determine the Cl_{th} of S–C systems with CIAs. This paper develops a suitable, short–term test (known as mACT test). This mACT test would be useful for the engineers to determine the Cl_{th} of S–C systems with CIAs in about 120 days (say, during the planning and design stage itself). This determined Cl_{th}, in turn, can be used to estimate the potential service life that could be achieved.

3 Experimental program

In this study, three phases of experiments were conducted.

- Phase-1: Study on the effect of external potential on the migration of chlorides and nitrites in cementitious systems. The Rapid Migration (RM) test was used.
- Phase-2: Development and validating of a 'modified' ACT (known as mACT herein) test procedure to determine the Cl_{th} of S–C systems with CIAs.
- Phase-3: Determination of the Cl_{th} of S–C systems with AN and BP type CIAs, using the mACT test method developed in Phase-2.

3.1 Phase-1: Effect of external potential on the migration of chlorides and nitrites through mortar

3.1.1 Rapid migration test setup

Figure 2a shows the schematic of ACT test setup to determine the Cl_{th} of steel embedded in plain mortar

[39]. In this, the steel specimen has a 15 mm thick mortar cover (indicated by the curly bracket), across which potential gradient of 20 V is applied. This scenario is simulated in the RM cell arrangement, which follows the test setup given in [40]. Figure 2b shows the schematic of the RM cell with a 15 mm thick mortar cylinder (100 mm diameter) sandwiched between the cells with sodium chloride (NaCl) solution and simulated pore solution (SPS). The positive terminal of the DC potential source was connected to the cell with SPS and the negative terminal to the cell with NaCl solution. Upon application of potential gradient across these terminals, the chlorides and nitrites would migrate. The rightward arrow in Fig. 2b indicates the direction of migration of chloride and nitrite ions (denoted as 'C' and 'N' in Fig. 2b. A photograph of the RM cell is shown in Fig. 2c.

3.1.2 Materials used

The mixture proportion of the mortar was 0.5:1:2.25 (water:cement:sand). Distilled water was used for the preparing the mortar. The 53-Grade Ordinary Portland Cement meeting the IS:12269 [41] and with a Blaine's fineness of 220 m^2/kg and specific gravity of 3.14 was used [42]. Silica sand of IS:383 Grades I, II and III (in 1:1:1 proportion) was used to make the mortar [43].

A calcium nitrite based AN type inhibitor (29% solid content) was used at a manufacturer recommended dosage of 5.4 ml/kg of cement. The cement mortar cylinders of size the 100 mm diameter and 200 mm length mortar cylinders were cast and cured for 28 days at standard laboratory condition. Then, the specimens were sliced to 15 mm length and used for RM tests.

3.1.3 Rapid migration test

The prepared 15 mm thick mortar cylinders were placed in the RM test cell as shown in Fig. 2b, c. The SPS contained 0.3, 10.4, and 23.23% of calcium hydroxide, Sodium hydroxide, potassium hydroxide, respectively. Then, an external potential of 20 V was applied continuously for 6, 12, 36, and 48 h. Three specimens each were tested for each duration (leading to a total of 12 specimens). At the end of the potential application for the specified periods, the mortar powder at a depth of 3, 7, 11, and 13 mm (from the mortar surface in contact with the 3.5% NaCl cell) was collected from each specimen. Then, the chloride concentrations in these powder samples were determined using the SHRP–330 procedure [44]. The nitrite concentrations in these powder samples were determined using the UV–Visible spectrometer. The ratio
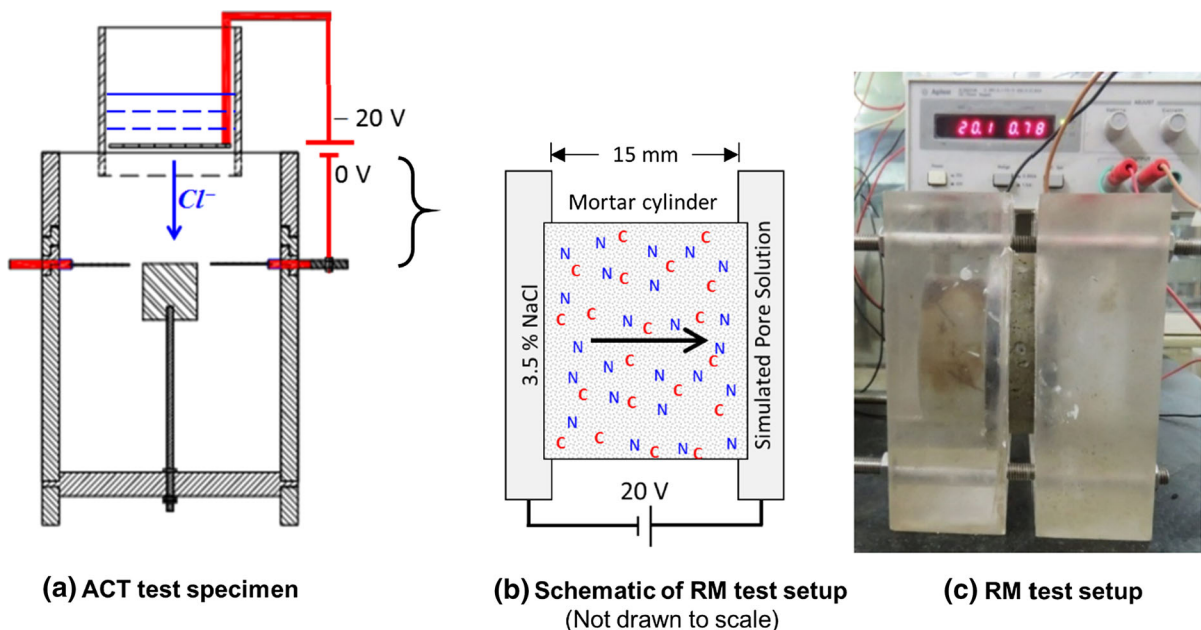

(a) ACT test specimen

(b) Schematic of RM test setup
(Not drawn to scale)

(c) RM test setup

Fig. 2 Comparison of ACT specimens with RMT test

between the chloride and nitrite ions (denoted as Cl/NO$_2$ herein) was also calculated.

3.2 Phase-2: Development of the mACT test procedure

The ACT test method [38, 39] was modified to mACT test method with the following features: (1) no application of potential gradient (2) reduced cover depth [from 38 to 15 mm], (3) increased concentration of NaCl solution [from 3.5 to 15%], and (3) modified statistical method to detect corrosion. Following sections present the details on: (i) specimen configuration and materials used (ii) casting, curing and exposure conditions, (iii) corrosion measurements, (iv) detection of corrosion initiation, and (v) determination of chloride concentration.

3.2.1 Specimen configuration and materials used

Figure 3 shows the schematic of the mACT test specimen and setup. The mACT moulds with features to appropriately place or embedded the various electrodes in the mortar were designed and fabricated. A 100 mm diameter Polyvinyl chloride (PVC) cylinder (Item 8 in Fig. 3) is the mould for holding the cement mortar. A 16 mm diameter steel rebar was cut to 20 mm length and used (Item 5) as working

electrode (WE). The chemical composition of the steel is shown in Table 2. The Ordinary Portland Cement was used to cast the specimens (see Table 2 for chemical composition). The standard silica sand classified as Grade III in IS:383 was used [43]. Mortar with cement:sand ratio of 1:2.25 and a water-cement ratio of 0.45 ± 0.05 was used. Distilled water was used for preparing the mortar. Eight 'without Inhibitor' specimens, were tested to develop and validate the mACT test method and determine the Cl_{th} of steel in plain mortar (i.e., without inhibitors).

3.2.2 Casting, curing, and exposure conditions

The mACT test specimens were cast according to the procedures given in Appendix A of Karuppanasamy [45]. The solution reservoir was filled with distilled water after the final setting time. The specimens were then cured for 28 days in a laboratory environment with $65 \pm 5\%$ relative humidity (RH) and 25 ± 2 °C temperature. After the curing period, the solution reservoir (Item 2) on the top of each specimen was filled with 15% sodium chloride solution (150 g of NaCl in 850 g of deionised water). The solution level was maintained at 30 mm above the mortar surface. The solution in the reservoir was replaced at an interval of 10 days with a freshly prepared solution to maintain the similar chloride concentration.
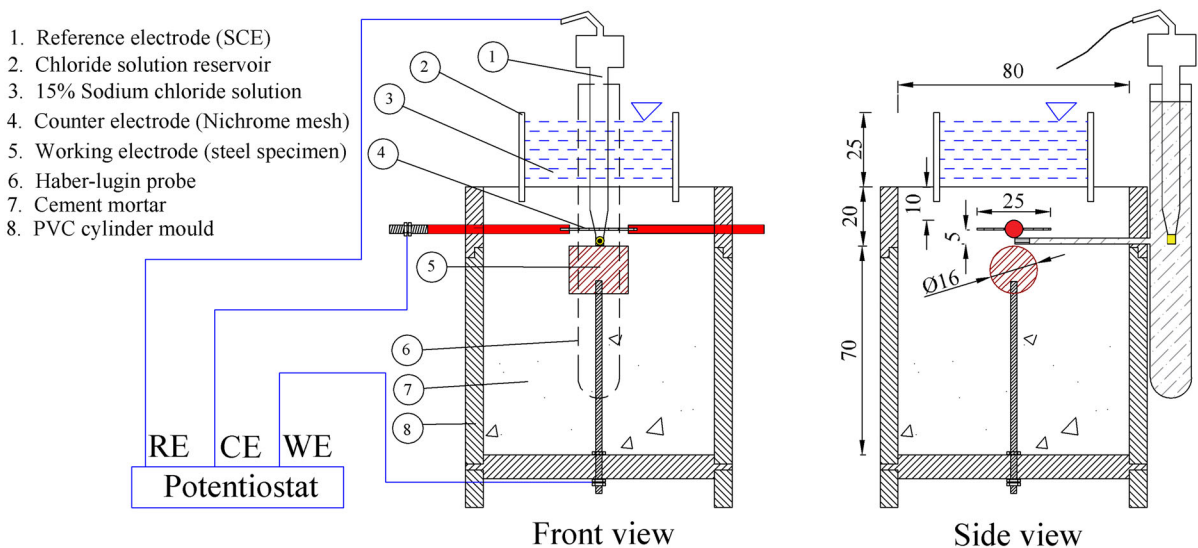

1. Reference electrode (SCE)
2. Chloride solution reservoir
3. 15% Sodium chloride solution
4. Counter electrode (Nichrome mesh)
5. Working electrode (steel specimen)
6. Haber-lugin probe
7. Cement mortar
8. PVC cylinder mould

Fig. 3 Modified accelerated chloride threshold (mACT) test layout

Table 2 Chemical compositions of QST steel and OPC used	Quenched and self-tempered (QST) steel		Ordinary portland cement (OPC)	
	Element	Constituents (%)	Element	Constituents (%)
	Cu	0.16	Al_2O_3	4.51
	Co	0.02	CaO	66.67
	Al	0.03	Fe_2O_3	4.94
	Ni	0.15	K_2O	0.43
	Mo	0.06	MgO	0.87
	Cr	0.24	Na_2O	0.12
	S	0.01	SiO_2	18.91
	P	0.08	SO_3	2.50
	Mn	0.63		
	Si	0.24		
	C	0.20		
	Fe	Remaining		

3.2.3 Corrosion measurements

As shown in Fig. 3, the test setup consists of three–electrode corrosion cell system (WE, CE, and RE). The Open Circuit Potential (OCP) and Linear Polarization Resistance (LPR) tests were conducted on each mACT specimen using an electrochemical workstation (Solartron Models—SI 1287/1260). At first, the OCP of WE was measured. Then, the LPR test was conducted by sweeping the potential from −15 to +15 mV with respect to OCP and at a scan rate of 0.1667 mV/s. Then, the electrical impedance spectroscopy (EIS) test with a stable AC potential of 10 mV and frequency ranging from 1 MHz to 0.1 Hz was conducted to determine the total resistivity (say, R_{total}) of the S–C interface and the thin mortar layer (say, about 2 mm) between the embedded reference electrodes (RE) and counter electrode (CE). The R_{total} was calculated as the slope of the applied potential (E) versus measured current density (i) curve at the zero-corrosion current and expressed mathematically as follows:

$$R_{total} = \left(\frac{\Delta E}{\Delta i} \right)_{E \to E_{corr}} \tag{3}$$

The bulk resistivity of the mortar layer between the electrodes (say, R_{cm}; the subscript 'cm' stands for cementitious material) was calculated by fitting the EIS data in the modified Randles circuit [46]. Based on the repeated testing of specimens, it was found that the R_{cm} value decreases as a function of the exposure period and becomes negligible by about 30 days of

exposure to chloride solution. Thus, the polarization resistance of S–C interface (R_p) can be assumed to be equal to R_{total}, as follows.

$$R_{total} \approx R_p \tag{4}$$

The R_p changes as a function of the change in corrosion activity. The R_p values are monitored at every 72 ± 3 h until the detection of corrosion initiation. To confirm the corrosion initiation, at least one more R_p is measured and analyzed. The following statistical approach was adopted to detect and define corrosion initiation.

3.2.4 Detection of corrosion initiation

Figure 4 shows the flowchart of the test procedure to conduct the mACT test and obtain Cl_{th}. Considering the large scatter in the corrosion data, the $(1/R_p)$ values observed at the beginning of the exposure period may have significant scatter, which can lead to erroneous interpretation of data. This randomness/scatter is shown in the early part of Fig. 5. Typically, the randomness reduces and the $(1/R_p)$ gets stabilized after about a month of exposure. In this study, a 'stable' set of five $(1/R_p)$ values (i.e., with acceptable scatter) is identified as follows.

First, the mean and standard deviation of the first five consecutive $(1/R_p)$ values (denoted as μ_5 and σ_5) are calculated. This data set is considered as 'stable' if all the five $(1/R_p)$ values are less than $(\mu_5 + k \sigma_5)$; the definition of k is provided in the next paragraph.
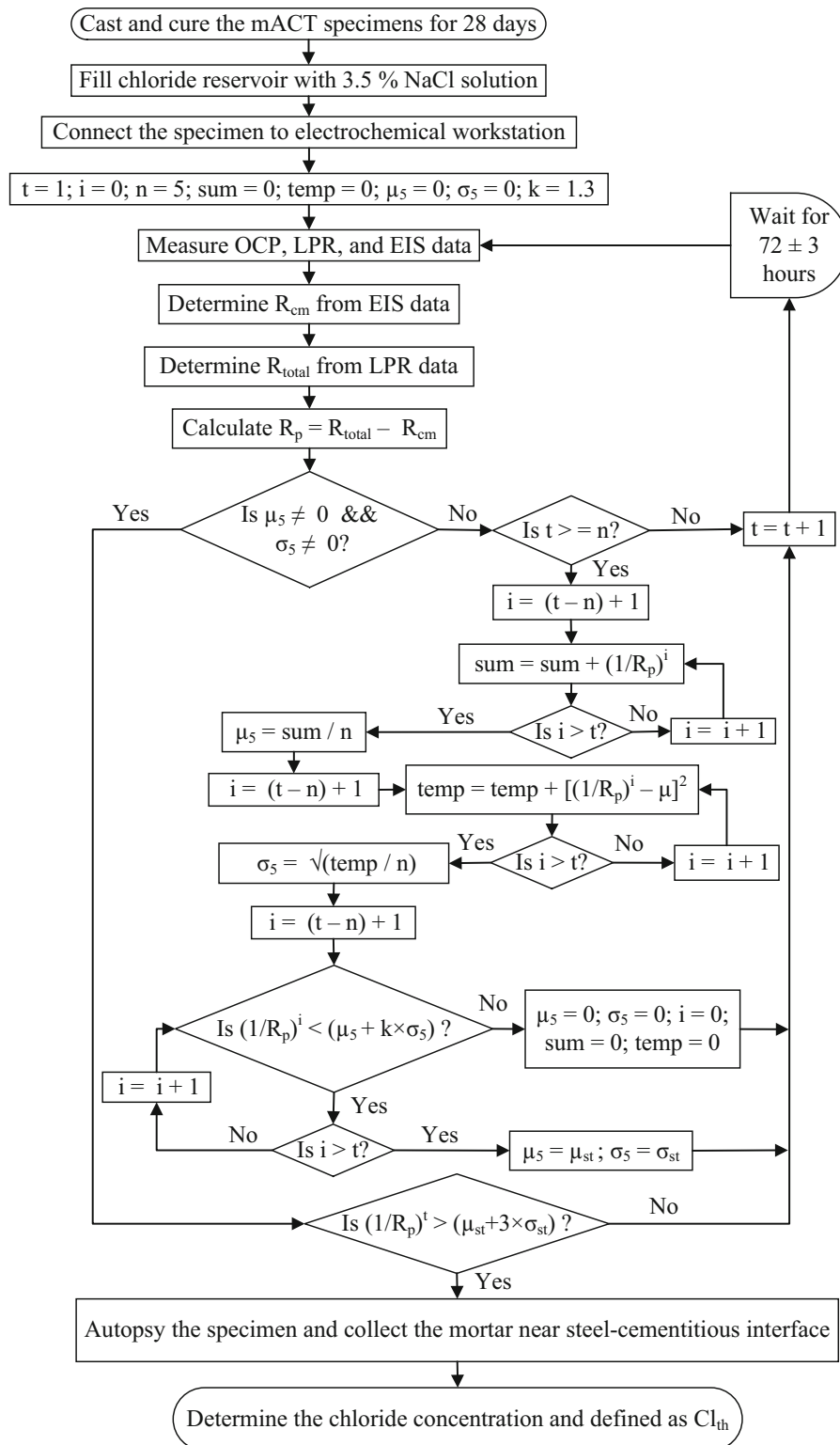
Fig. 4 Flowchart to conduct mACT test

Otherwise, the next five consecutive $(1/R_p)$ values are checked for the stable data condition. This will be continued until a stable data set is identified. Once the stable $(1/R_p)$ data set is identified, the corresponding μ_5 and σ_5 are defined as μ_{st} and σ_{st}). In short, the stable data limit is shown by the horizontal line with cross markers [i.e., at $(\mu_{st} + 1.3\ \sigma_{st})$] in Fig. 5. Then, the LPR tests are continued until the corrosion initiation occurs. Corrosion initiation is defined to occur when the $(1/R_p)$ value exceeds the $(\mu_{st} + 3\sigma_{st})$. This statistical approach was followed for detecting corrosion of each specimen.

The value of k was determined using a different analysis on $(1/R_p)$ values (not discussed in detail in this document). It was found that $k = 1.3$ yielded reasonable number of test specimens with 'stable' data set. When the k-value was less than 1.3, many specimens did not exhibit 'stable' data set. On the other hand, keeping the k-value above 1.3 led to other challenges in detecting corrosion initiation. In short, $k = 1.3$ was found suitable and used in this study. More details on the determination of k are given in Karuppanasmy [45].

3.2.5 Determination of chloride concentration

Once the corrosion is initiated, the specimens are autopsied at the level of the mortar between the steel surface and Luggin probe, as shown in Fig. 6. It should be noted that in most cases, the specimens may not exhibit visible corrosion. In other words, the corrosion initiation was detected before significant qua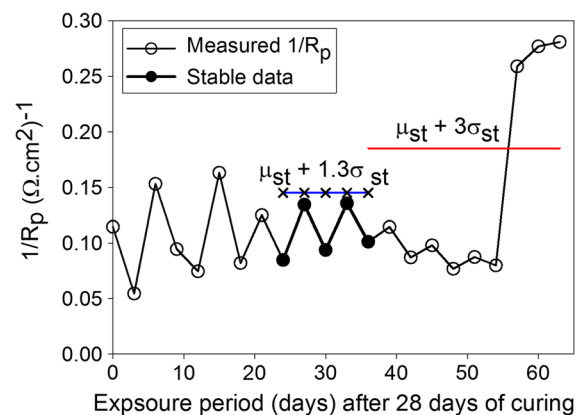ntity of rust that is visible with naked eyes was formed. In some cases, very small rust spots were observed at or near the ribs and away from the epoxy coating. The mortar adjacent to the steel surface was powdered using the profile grinder (Fig. 6 shows the location of grinding) and the chloride concentration was determined, as per SH*RP*–330 procedure [44]. This chloride concentration is defined as the Cl_{th} of the S–C system. Additional details about the mACT test are provided in Karuppanasmy [45].

3.3 Phase-3: Determination of Cl_{th} of QST embedded in AN and BP corrosion inhibitors

The pu*R*$_p$ose of the mACT method is to determine the effect of AN and BP type CIAs on the Cl_{th} of Quenched and Self–Tempered (QST) (or Thermo–Mechanically Treated (TMT)) steel embedded in cementitious systems. In this study, a total of 30 mACT test specimens with QST steel pieces embedded in mortar without inhibitors ('W/O') and with anodic and bipolar inhibitors ('AN' and 'BP') were tested (i.e., 10 specimens each of W/O, AN, and BP). The manufacturer recommended dosage of 5.4 ml/kg of cement was adopted for the calcium nitrite based AN inhibitor. The manufacturer recommended dosage of 5 ml/kg of cement was adopted for the BP inhibitor with calcium nitrite and amino alcohol.

4 Results and discussions

4.1 Phase-1: Effect of external potential on the migration of anions through mortar

Figure 2 shows the schematic and photograph of the Rapid Migration (RM) test setup used for this study.

Fig. 5 Statistical approach used in mACT method to detect corrosion initiation

Fig. 6 Specimen autopsied across the steel mortar interface

The change in the concentration of anions near the SPS cell (at right side) is the focus of this study (i.e., at 13 mm from the chloride solution cell). The changes in the concentrations of chlorides and nitrites, and the chloride-nitrite ratio at various depths in mortar, due to the application of potential gradient, are discussed next.

4.1.1 Migration of chloride ions

Figure 7a shows the chloride concentration (in %bwoc; by weight of cement) at different depths of the 15 mm thick mortar specimens exposed to the external potential of 20 V for 6, 12, 36, and 48 h. The concentration of chlorides in the mortar near the SPS cell is about 0.7 %bwoc after 6 h of potential application (circular markers at right end). The concentration of chlorides increases almost linearly with increase in the duration of potential applied. After 48 h of potential application, chloride concentration in the mortar near the SPS cell (at right end) increases to about 1.1 %bwoc (triangular marker). Thus, the external potential application results in the migration of chlorides through mortar within a short duration. However, it also helps in the migration of nitrite ions, as discussed next.

4.1.2 Migration of nitrite ions

Figure 7b shows the concentration of nitrites at different depths in mortar with respect to the duration of application of 20 V. The concentration of nitrites in mortar near the SPS cell is about 0.3 %bwoc even after 12 h of potential application (see the square marker at right end). However, this concentration has increased to about 1.2 %bwoc after 48 h of potential application (see the triangular marker at right end). These results prove that the concentration of nitrites near the steel WE in the ACT test specimen would increase significantly if the external potential is applied for long term. This increased nitrite concentration at the steel surface can lead to a delay in corrosion initiation—but, such increase in nitrite concentration will not happen in real structures. Therefore, it can be concluded that the application of external potential can lead to erroneous estimation of the Cl_{th} of S–C systems with CIAs containing anions.
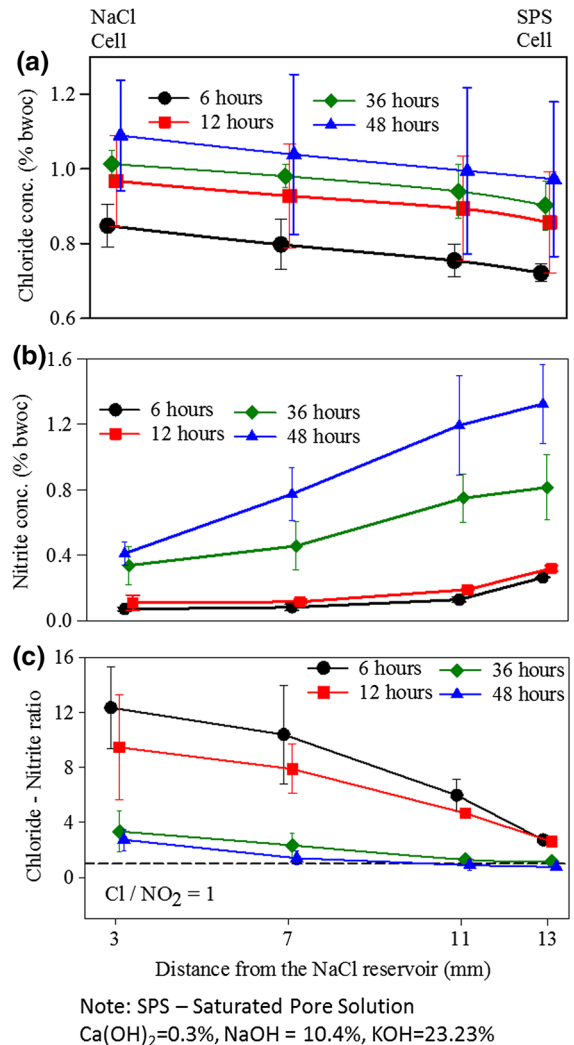

Fig. 7 Variation in (**a**) chloride concentration, (**b**) nitrite concentration, and (**c**) chloride-to-nitrite ratio due to application of external potential (20 V)

4.1.3 Variation in the chloride-nitrite ratio

Figure 7c shows the Cl/NO_2 ratio at different depths in mortar with respect to the duration of application of 20 V (i.e., 6, 12, 36, and 48 h). With the increase in the duration of application of 20 V, the Cl/NO_2 ratio reduces to a value below one (triangular and rhombus markers), which is reported as the threshold value for corrosion initiation [5]. Also, the change in this ratio depends on the rate of change of either Cl^- or NO_2 concentrations (i.e., either numerator or denominator). This indicates that due to the prolonged application of

potential gradient, the concentrations of both chlorides and nitrites at the steel surface could increase significantly, but at the same time it may not exhibit active corrosion because the Cl/NO_2 ratio is less than one.

Based on these, it can be concluded that the external potential can be used to accelerate the chloride in plain mortar (as in the ACT test [39]). However, it is not suitable to accelerate chlorides for testing Cl_{th} of in systems with CIAs containing anions. In short, the application of an external potential to drive the chlorides towards the surface of the embedded steel alters the S–C interface chemistry and provide erroneous test results. Thus, an alternate Cl_{th} test method, which will not alter the anion concentrations near the steel surface during the course of the testing is required to assess the Cl_{th} of systems with CIAs containing various anions.

4.2 Phase-2 mACT test results

4.2.1 Inverse polarization resistance data for specimens without inhibitors

Figure 8a shows the variation of inverse polarization resistance ($1/R_p$) as a function of exposure period for specimens without (W/O) inhibitors. The unfilled circular marker towards the end of each curve indicates the corrosion initiation point for that particular specimen. Corrosion initiation was detected using the method discussed earlier in this paper. For example, Specimen W/O-S8 exhibits a significant increase in ($1/R_p$) at about 30 days of exposure. Similarly, other specimens also showed corrosion initiation between about 24 and 36 days. Two W/O specimens showed significant scatter in the $1/R_p$ values. The reason for this unexpected behaviour could not be identified. Also, due to this, the identification of stable data was difficult as per the statistical approach provided in Sect. 3.2.4. Thus, only eight out of ten specimens were used for further analysis and interpretation in this study. The measurements were continued for at least one more reading after the circular markers. This was done so to confirm that the active corrosion is propagating. In general, all specimens showed corrosion initiation in reasonable period of time.
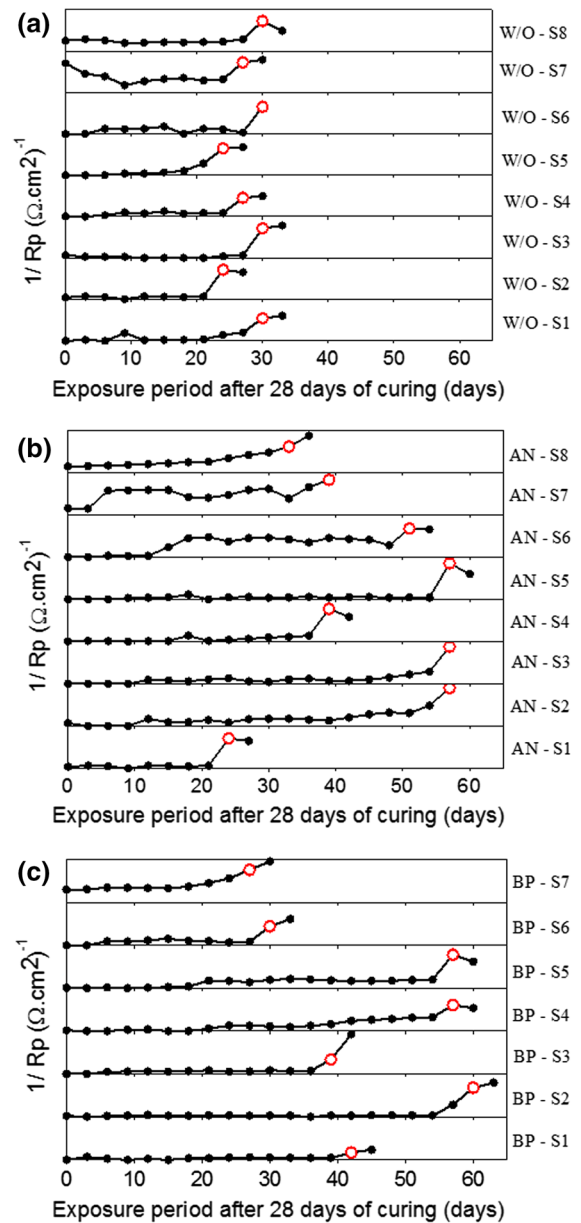

Fig. 8 Inverse polarization resistance Vs chloride exposure time for systems with (**a**) W/O inhibitor, (**b**) AN inhibitor, and (**c**) BP inhibitor

4.2.2 Cl_{th} for specimens without inhibitor and validation of mACT test method

The second column in Fig. 9 shows the Cl_{th} of steel embedded in cementitious systems without inhibitors (determined using the mACT test method). The average Cl_{th} of the steel is found to be about

1.0 %bwoc (indicated by the solid horizontal line) and the standard deviation is 0.5 %bwoc. To validate the developed mACT test method, it would be ideal to compare the determined Cl_{th} values with those determined using a long-term test method with the identical S–C systems. However, such tests could not be performed. Therefore, the Cl_{th} values (for S–C systems without inhibitors) reported in the literature over a period of 50 years (see Fig. 1) were collected and compared with the results obtained from the mACT method. The data points shown in the first column of Fig. 9 are the average Cl_{th} values reported in the literature and is about 0.8% by weight of cement (%bwoc) and standard deviation of 0.4 %bwoc.

Statistical tests were performed on these two data sets for specimens without inhibitor case. Both the Cl_{th} data reported in the literature and those determined using the mACT test method passed the normality test (Shapiro—Wilkinson method). Further, Student's t-test using the two data sets concluded that, at a significance level of $\alpha = 0.05$, there is no evidence to reject the null hypothesis. This indicates that there is a statistical similarity between the two data sets in 1st and 2nd columns of Fig. 9. This validates that the mACT test can produce good estimates of Cl_{th} for high relative humidity conditions (say about 95–100%) because this test adopted a continuous ponding with NaCl solution. Also, while autopsying the mACT specimens, it was visually observed that the water saturation level at the S–C interface was between 95 and 100%—resulting in the average Cl_{th} values of abound 1.0 %bwoc, which is in good agreement with the findings by Pettersson. Pettersson reported that the

average Cl_{th} observed for systems with 0.5 w/c mortar at 95% relative humidity was about 0.8 %bwoc [47].

4.3 Phase-3: Determination of chloride threshold of steel embedded in systems with CIAs

This subsection provides the Cl_{th} of eight specimens each with steel embedded in cementitious systems with AN and BP inhibitors. Similar to the case of without inhibitors, the variation of $(1/R_p)$ as a function of exposure period for specimens with 'AN', and 'BP' inhibitors (Fig. 8b, c), respectively is considered for detecting the corrosion initiation.

4.3.1 Cl_{th} of steel embedded in systems with CIAs

The second, third, and fourth column of the Fig. 9 shows the Cl_{th} values of steel embedded in mortar with W/O, AN, and BP inhibitors. Table 3 shows the Cl_{th} values obtained for each specimen. The Cl_{th} of steel embedded in cementitious system with W/O, AN, and BP inhibitors can be expressed as normal distributions as follows: $\sim N(1.0, 0.5)$, $\sim N(1.4, 0.35)$, and $\sim N(1.8, 0.6)$ %bwoc, respectively. The average Cl_{th} of specimens with CIAs exhibited higher Cl_{th} values than that of specimens without inhibitors shown in Column 1. Moreover, the Cl_{th} values of many specimens with BP inhibitors are higher than the average Cl_{th} of the specimens without inhibitor and AN inhibitor.

4.3.2 Duration of mACT testing for systems with and without CIAs

The exposure period (after 28 days of curing) required for specimens to initiate corrosion on the steel when embedded in cementitious systems with different CIAs is calculated. The mACT specimens without inhibitor took about 28 days to initiate corrosion. The mACT specimens with AN and BP took an average of 42 and 54 days, respectively, to initiate corrosion. Based on these results, it can be concluded that the average time required to initiate corrosion will be around 70 days. It indicates that the total time (including specimen preparation, casting, curing, etc.) to determine the Cl_{th} using the developed mACT test method could be around 4 months. Therefore, the mACT test method could be used to determine Cl_{th} of
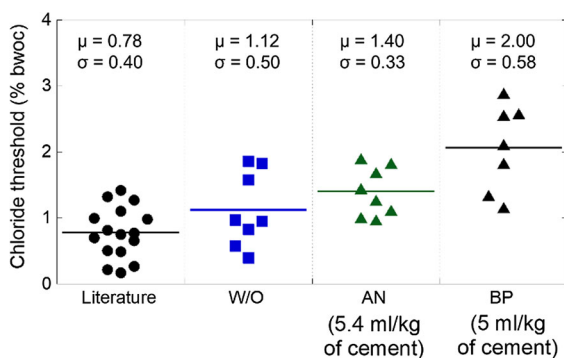

Fig. 9 Chloride threshold of QST steel in systems with and without CIAs

Table 3 Chloride threshold of QST steel in cementitious system with and without CIAs

Specimen number	Cl_{th} of steel in mortar with		
	W/O	AN	BP
S1	0.40	1.01	1.83
S2	0.58	1.39	2.12
S3	0.96	1.83	2.56
S4	1.14	1.90	1.34
S5	1.83	1.39	1.38
S6	0.83	1.12	1.76
S7	1.58	1.45	2.58
S8	1.01	0.97	No data
Equivalent normal distribution, $\sim N(\mu, \sigma)$	$\sim N(1.0, 0.48)$	$\sim N(1.4, 0.35)$	$\sim N(1.9, 0.51)$

systems with new steel and CIAs and estimate service life during the planning and design stage itself.

5 Practical Applications of the mACT

The main focus of this study is to facilitate the assessment of the effect of CIAs in increasing the overall service life of structures by increasing the corrosion initiation period (t_i). In the present study, t_i for a reinforced concrete column made of OPC concrete ($w/b = 0.5$) with a cover depth of 50 mm and different CIAs are estimated using Life–365^{TM} software program [48]. The Cl_{th} values for systems with different CIAs determined using the mACT test method were used. The chloride diffusion coefficient of concrete was assumed to be 2×10^{-12} m^2/s [49, 50]. The probability density functions (PDFs) of the t_i for the three systems (with W/O, AN, and BP inhibitors) are shown in Fig. 10. The vertical lines within each PDF indicate the median of the estimated t_i [denoted as $M(t_i)$]. The systems without inhibitors may exhibit an $M(t_i)$ of 28 years, whereas the systems with AN and BP inhibitors could exhibit an $M(t_i)$ of 37 and 51 years, respectively. Also, in Fig. 10, note that the scatter of the PDF for the cases with anodic and bipolar inhibitors is larger than that for the case without inhibitor. This is because the LIFE–365^{TM} software program assumes a constant Coefficient of Variation of 0.2 for the chloride threshold. This indicates that the larger the mean value of Cl_{th}, the larger will be the standard deviation calculated by Life–365^{TM}. This larger standard deviation leads to a larger scatter of the PDF as the mean of the Cl_{th}
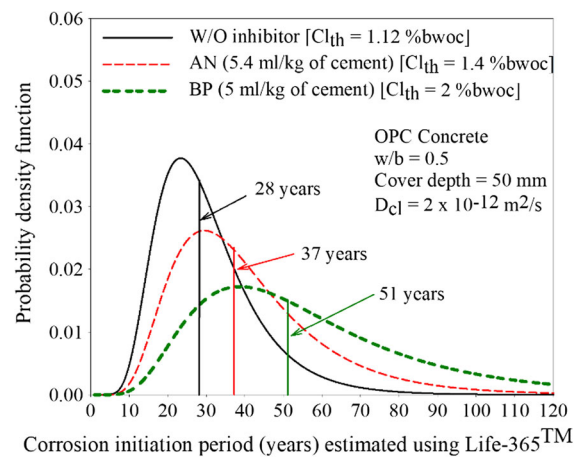

Fig. 10 Estimated corrosion initiation period of steel with different CIAs

increases. However, it should be noted that the experimental values observed in this test program (with less than 10 specimens in each case) did not exhibit a systematic increase in the scatter as the mean Cl_{th} increased. A software program that considers a user-defined COV for Cl_{th} needs to be developed for estimating the service life in a more realistic manner.

6 Limitations of mACT test method and future work

- *Specimen size* The length of steel specimen used for the study is only 20 mm. Such a small specimen may not sometimes allow sufficient cathodic area to be developed to sustain the active corrosion. This could lead to a longer time for

corrosion initiation and the subsequent active corrosion rates could be lower [51]. However, note that this test adopts repeated measurements of instantaneous corrosion rates on same specimen (similar to a typical metallographic specimen) and statistical comparison to detect if there are any statistically significant changes. Therefore, the results may still be reasonable. Further studies are required to quantify the effect of the specimen size and electrode configuration.

- *Specimen preparation* It is very crucial to ensure that the distance between the electrodes in the 3-electrode mACT specimen is maintained as prescribed. This requires a delicate, careful, and meticulous approach of casting the specimen. Also, the epoxy used for coating the side faces of the steel specimen must be very good and resistant to alkaline environment—so that the chances of underfilm/crevice corrosion in minimal.

- *Test procedure* The mACT procedure detects the corrosion initiation by conducting the repeated LPR tests followed by a statistical approach. The data analysis involved in this process may be complex for some technicians.

- *Application* The determined Cl_{th} might be suitable only for the structures experiencing high moisture conditions (say, submerged or saturated conditions). The direct application of the results to other moisture conditions may be appropriate. However, Frederickson (1996) provides useful information for such extrapolations [52].

7 Conclusions

The following conclusions were drawn from this experimental work.

- The application of external potential is not a suitable method to accelerate the chlorides towards the embedded steel in a chloride threshold test; the determined Cl_{th} of S–C system with CIAs may be erroneous.

- A new test method is developed for determining Cl_{th} of S–C systems with CIAs containing anions. The time required to complete the test is about 3 months. However, it should be noted that the better the inhibitors under evaluation, the longer would be the test duration.

- The specimens without inhibitors exhibited Cl_{th} of 1.0 ± 0.5 %bwoc, which is similar to the range of the reported values in the literature (0.8 ± 0.4 %bwoc). Considering the inherent variations in corrosion mechanisms and large scatter in measurements reported in the literature, it could be concluded that the modified ACT test is a suitable test procedure.

- The specimens with anodic and bipolar inhibitors exhibited Cl_{th} of 1.4 and 1.8 %bwoc, respectively. Based on this, it can be concluded that the use of CIAs can potentially delay the onset of corrosion in concrete structures in immersed conditions.

- For a system with a cover depth of 50 mm and chloride diffusion coefficient of 2×10^{-12} m^2/s, the use of anodic and bipolar CIAs can delay the corrosion initiation period by about 1.5 and 2 times, respectively; when compared to that of steel embedded in the cementitious system without any corrosion inhibitor.

- Note that the results in this paper are for Portland cement mortar systems with a w/c ratio of 0.50. The times to corrosion initiation would be significantly increased for steel in concrete and for lower w/c ratios. Furthermore, the addition of supplementary cementitious materials could alter the pore solution composition and the chloride threshold, the influence of inhibitors and the time to initiate corrosion.

Compliance with ethical standards

References

1. Trejo D, Reinschmidt K (2003) High-performance construction materials for life-cycle optimization. Construction research congress, Honolulu, Hawaii, March 19–21

2. Yu H, Hartt WH (2011) Correction of chloride threshold concentration and time-to-corrosion due to reinforcement presence. Mater Corros 62(5):423–430

3. Cheewaket T, Jaturapitakkul C, Chalee W (2012) Initial corrosion presented by chloride threshold penetration of concrete up to 10 year-results under marine site. Constr Build Mater 37:693–698

4. Pillai RG, Annapareddy A (2013) Service life models for chloride-laden concrete structures: a review and nomographs. Int J 3Rs 4 (2): 563–580

5. Gaidis JM (2004) Chemistry of corrosion inhibitors". Cement Concr Compos 26(3):181–189

6. Ann KY, Song HW (2007) Chloride threshold level for corrosion of steel in concrete. Corros Sci 49:4113–4133

7. Xu J, Jiang L, Wang W, Jang Y (2011) Influence of $CaCl_2$ and NaCl from different sources on chloride threshold value for the corrosion of steel reinforcement. Constr Build Mater 25(2):663–669

8. Taylor PC, Mohammad AN, David AW (1999) Threshold chloride content for corrosion of steel in concrete: a literature review. Portland cement Association, R&D, Serial No. 2169

9. Angst U, Elsener B, Larsen CK, Vennesland O (2009) Critical chloride content in reinforced concrete—a review. Cem Concr Res 39(12):1122–1138

10. Hansson CM, Mammoliti L, Hope BB (1998) Corrosion inhibitors in concrete—part I: the principles. Cem Concr Res 28(12):1775–1781

11. Ormellese M, Berra M, Nolzoni F, Pastore T (2006) Corrosion inhibitors for chlorides induced corrosion in reinforced concrete structures. Cem Concr Res 36:536–547

12. Morris W, Vazquez M (2002) Migrating corrosion inhibitor evaluated in concrete containing various contents of admixed chlorides. Cem Concr Res 32:259–267

13. González JA, Ramírez E, Bautista A (1998) Protection of steel embedded in chloride-containing concrete by means of inhibitors. Cem Concr Res 28(4):577–589

14. Mammoliti L, Hansson CM, Hope BB (1999) Corrosion inhibitors in concrete part II: effect on chloride threshold values for corrosion of steel in synthetic pore solutions. Cem Concr Res 29:1583–1589

15. Ann KY, Jung HS, Kim HS, Kim SS, Moon HY (2006) Effect of calcium nitrite-based corrosion inhibitor in preventing corrosion of embedded steel in concrete. Cem Concr Res 36:530–535

16. Berke NS, Hicks MC (2004) Predicting long-term durability of steel-reinforced concrete with calcium nitrite corrosion inhibitor. Cem Concr Compos 26(3):191–198

17. Page CL, Treadaway KWJ, Bamforth PB (1990) The use of calcium nitrite as a corrosion inhibiting admixture to steel reinforcement in concrete. Elsevier Applied Science, London, New York, pp 571–585

18. Rincon TO, Perez O, Paredes E, Caldera Y, Urdaneta C, Sandoval I (2002) Long-term performance of ZnO as a rebar corrosion inhibitor. Cem Concr Compos 24(1):79–87

19. Montes P, Bremner TW, Lister D (2004) Influence of calcium nitrite inhibitor and crack width on corrosion of steel in high performance concrete subjected to a simulated marine environment. Cem Concr Compos 26:243–253

20. Nmai CK (2004) Multi-functional organic corrosion inhibitor. Cem Concr Compos 26(3):199–207

21. COIN Project report 22 (2010) Corrosion inhibitors—state of the art. SINTEF Building and Infrastructure

22. Rakanta E, Zafeiropoulou T, Batis G (2013) Corrosion protection of steel with DMEA-based organic inhibitor. Constr Build Mater 44:507–513

23. Nmai CK, Farrington SA, Bobrowske GS (1992) Organic-based corrosion-inhibiting admixture for reinforced concrete. Concr Int 14(4):45–51

24. Pour-Ghaz M, Isgor OB, Ghods P (2009) Quantitative interpretation of half-cell potential measurements in concrete structures. J Mater Civ Eng 21(9):467–475

25. Stratfull RF (1957) The corrosion of steel in a reinforced concrete bridge. Corrosion 13:173

26. ASTM C876–2015, Standard test method for corrosion potentials of uncoated reinforcing steel in concrete. American standards for testing of materials, 100 Barr Harbor Drive, West Conshohocken, PA 19428-2959, United States

27. Cigna R, Proverbio E, Rocchini G (1993) A study of reinforcement behavior in concrete structures using electrochemical techniques. Corros Sci 35(5–8):1579

28. ASTM G59-14. Standard test method for conducting potentiodynamic polarization resistance measurements. American standards for testing of Materials, 100 Barr Harbor Drive, West Conshohocken, PA 19428-2959, United States

29. Baweja D, Roper H, Sirivivatnanon V (2003) Improved electrochemical determinations of chloride-induced steel corrosion in concrete. ACI Mater J Tech Pap 100:547–584

30. Morris W, Vico A, Vazquez M, de Sanchez S (2002) Corrosion of reinforcing steel evaluated by means of concrete resistivity measurements. Corros Sci 44(1):81–99

31. Xu J, Jiang L, Wang J (2009) Influence of detection methods on chloride threshold value for the corrosion of steel reinforcement. Constr Build Mater 23(5):1902–1908

32. Bouteiller V, Cremona C, Baroghel-Bouny V, Maloula A (2012) Corrosion initiation of reinforced concretes based on Portland or GGBS cements: chloride contents and electrochemical characterizations versus time. Cem Concr Res 42(11):1456–1467

33. Angst UM, Elsener B, Larsen CK, Vennesland Ø (2011) Chloride induced reinforcement corrosion: electrochemical monitoring of initiation stage and chloride threshold values. Corros Sci 53(4):1451–1464

34. Valipour M, Shekarchi M, Ghods P (2014) Comparative studies of experimental and numerical techniques in measurement of corrosion rate and time-to-corrosion-initiation of rebar in concrete in marine environments. Cement Concr Compos 48:98–107

35. JIS A6205 (2013) Corrosion inhibitor for reinforcing steel in concrete. Japan Industrial standard, 4-1-24, Akasaka, Minato-ku, Tokyo, 107-8440, Japan

36. Poursaee A, Hansson CM (2007) Reinforcing steel passivation in mortar and pore solution. Cem Concr Res 37(7):1127–1133

37. ASTM G109–15 (2015) Standard test method for determining effects of chemical admixtures on corrosion of embedded steel reinforcement in concrete exposed to chloride environments. American standards for testing of Materials, 100 Barr Harbor Drive, West Conshohocken, PA 19428-2959, United States

38. Trejo D, Miller D (2002) System and method for determining the chloride corrosion threshold level for uncoated steel reinforcement embedded in cementitious material. US Patent Application, Serial No. 60/288,210

39. Trejo D, Pillai RG (2003) Accelerated chloride threshold testing: part I ASTM A615 and A706 reinforcement. ACI Mater J 100:519–527

40. ASTM C1202 (2010) Standard test method for electrical indication of concrete's ability to resist chloride ion penetration, American standards for testing of materials, 100 Barr Harbor Drive, West Conshohocken, PA 19428–2959, United States

41. IS:12269-2008, Specification for 53 grade ordinary Portland cement, Bureau of Indian Standards (BIS), New Delhi, India

42. IS:4031-2008 (Part 1–15), Methods of physical tests for hydraulic cement, Bureau of Indian Standards (BIS), New Delhi, India

43. IS:383-1970 (2007) Specification for coarse and fine aggregates from natural sources for concrete. Bureau of Indian Standards (BIS), New Delhi, India

44. SHRP-330 (1993) Standard test method for chloride content in concrete using the specific ion probe. In Condition evaluation of concrete bridges relative to reinforcement corrosion-volume 8: procedure manual, SHRP-S/FR-92-110, Strategic Highway Research Program, Washington, DC, USA, pp. 85–105

45. Karuppanasamy J (2017) Study of chloride threshold determination for systems with corrosion inhibiting admixtures and corrosion rates of various steels in cement mortar. Ph.D. thesis, Indian Institute of Technology Madras, India

46. Feliu V, González JA, Andrade C, Feliu S (1998) Equivalent circuit for modeling the steel-concrete interface. I. Experimental evidence and theoretical predictions. Corros Sci 40(6):975–993

47. Pettersson K (1996) Factors influencing chloride induced corrosion of reinforcement in concrete. Durab Build Mater Compon 1:334–341

48. Life-365^{TM} v2.2.1, Life-365 Consortium III, Silica Fume Association, Lovettsville, www.life-365.org, 2014

49. Polder RB (1995) Chloride diffusion and resistivity testing of five concrete mixes for marine environment, RILEM International conference, Chloride Penetration into Concrete, Paris

50. Luping T, Nilsson LO (1992) Chloride diffusivity in high strength concrete at different ages. Nord Concr Res 11(1):162–171

51. Angst U, Rønnquist A, Elsener B, Larsen CK, Vennesland Ø (2011) Probabilistic considerations on the effect of specimen size on the critical chloride content in reinforced concrete. Corros Sci 53(1):177–187

52. Frederiksen JM (ed) (1996) HETEK. In Chloride penetration into concrete, state of the art. Transport processes, corrosion initiation, tests methods and prediction models, Copenhagen: The Road Directorate. Report No. 53

53. Montemor M, Simões AM, Ferreira MG (2003) Chloride-induced corrosion on reinforcing steel: from the fundamentals to the monitoring techniques. Cem Concr Compos 25(4):491–502

54. Pradhan B, Bhattacharjee B (2009) Half-cell potential as an indicator of chloride-induced rebar corrosion initiation in RC. J Mater Civil Eng 21(10):543–552

55. Yu H, Shi X, Hart WH, Lu B (2010) Laboratory investigation of reinforcement corrosion initiation and chloride threshold content for self-compacting concrete. Cem Concr Res 40(10):1507–1516

56. Boubitsas D, Tang L (2015) The influence of reinforcement steel surface condition on initiation of chloride induced corrosion. Mater Struct 48(8):2641–2658